ELSEVIER

Chemical Engineering Journal 135S (2008) S153–S158

Chemical Engineering Journal

www.elsevier.com/locate/cej

Gas hold-up and liquid film thickness in Taylor flow in rectangular microchannels

M.J.F. Warnier, E.V. Rebrov, M.H.J.M. de Croon, V. Hessel, J.C. Schouten *

Department of Chemical Engineering and Chemistry, Eindhoven University of Technology, P.O. Box 513, 5600 MB Eindhoven, The Netherlands

Abstract

The gas hold-up in nitrogen/water Taylor flows in a glass microchannel of rectangular cross-section (100 μm × 50 μm) was shown to follow the Armand correlation. The validity of the Armand correlation implies that the liquid film thickness is not a function of the bubble velocity, which was varied between 0.24 and 7.12 m/s. Images of the Taylor flow were captured at a rate of 10,000 frames per second and were used to obtain the bubble and liquid slug lengths, the bubble velocity, and the number of bubbles formed per unit of time. A mass balance-based model was developed for Taylor flow with negligible liquid film velocities. The model describes the gas hold-up as a function of the liquid film thickness, the bubble and liquid slug lengths, the liquid superficial velocity, and the bubble formation frequency.

Keywords: Taylor flow; Gas hold-up; Microchannel; Liquid film

1. Introduction

Taylor flow is the main flow regime of interest for performing gas/liquid/solid reactions in small channels (diameter <1 mm). It consists of sequences of a gas bubble and a liquid slug. The length of the gas bubbles is larger than the channel diameter and a thin liquid film separates the gas bubbles from the channel walls. The liquid film ensures a short diffusion path length for the gas phase diffusing through the film to the channel wall, where the catalyst is often located. The liquid in the slugs forms circulation cells when the capillary number ($Ca = \mu u_b/\sigma$) is smaller than 0.5 [1,2]. The circulation patterns within the liquid slugs improve radial mass transfer in the liquid as compared to laminar flow [3]. The thin liquid film and the liquid circulation cells make Taylor flow a suitable flow regime for three-phase reactions where mass transfer to the wall is of influence on the reaction rate.

The thickness of the liquid film and the liquid velocity therein are key parameters, not only for mass transfer, but also for describing the hydrodynamics of Taylor flow. The gas hold-up is an important parameter in reactor design since it determines the mean residence times of the phases in the reactor and is related to the thickness of the liquid film. Due to the presence of the liquid film, the gas bubbles move through a smaller cross-sectional area than the combined gas and liquid flows. Continuity then requires that the velocity of the gas bubbles is larger than the total superficial velocity in the channel. Because of this, the gas hold-up differs from the flow quality, which is defined as the volumetric fraction of gas in the feed stream. The relation between film thickness and gas hold-up also depends on the flow rate of the liquid in the film.

Bretherton [4] showed that the film thickness is a function of the capillary number for capillaries with a circular cross-section. Kolb and Cerro [2] expanded on this work by analyzing Taylor flow in tubes of square cross-section, also showing the film thickness to be a function of capillary number. However, these observations are only valid when inertia does not play a significant role. The conditions in small reactor channels operated in Taylor flow are often such that inertia has to be accounted for when estimating the film thickness. When taking inertia into account, it is reported that the film thickness is a function of both the capillary and Reynolds ($Re = \rho u_b W_b^2/\mu$) numbers and is therefore dependent on the bubble velocity [5–7]. Aussillous and Quere [5] found that inertial effects give rise to a thicker liquid film than predicted by Bretherton's theory and provide a qualitative explanation for this effect. They also stated that the thickening effect is superimposed by a geometric effect which makes the film thickness converge to a finite fraction of the tube radius. However, they provide no quantitative analysis for predicting this limit in the film thickness.

* Corresponding author. Tel.: +31 40 247 2850; fax: +31 40 244 6653.
E-mail address: j.c.schouten@tue.nl (J.C. Schouten).
URL: www.chem.tue.nl/scr (J.C. Schouten).

1385-8947/$ – see front matter © 2007 Elsevier B.V. All rights reserved.
doi:10.1016/j.cej.2007.07.008

Nomenclature

A	area of the channel cross-section (m^2)
A_b	area of the bubble cross-section (m^2)
Bo	Bond number
Ca	capillary number
F_b	frequency of bubbles (1/s)
g	gravitational constant (m/s^2)
L_b	length of a bubble (m)
L_{nose}	length of the nose of a gas bubble (m)
L_s	length of a liquid slug (m)
L_{tail}	length of the tail of a gas bubble (m)
Re	Reynolds number
u_b	velocity of a bubble (m/s)
U_g	superficial gas velocity (m/s)
U_l	superficial liquid velocity (m/s)
V_b	volume of a gas bubble (m^3)
V_f	volume of the liquid film in a unit cell (m^3)
V_s	volume of a liquid slug (m^3)
V_{uc}	volume of a unit cell (m^3)
W_b	width of the gas bubble (m)
We	Weber number

Greek symbols

δ	correction of slug length for the liquid in the slug surrounding the nose and tail of bubble (m)
ε_g	gas hold-up
μ	viscosity of the liquid (Pa s)
ρ	density of the liquid (kg/m^3)
σ	surface tension (N/m)

Experimentally determining the liquid film thickness or gas hold-up from images of the flows is difficult, especially for channels with a rectangular cross-section and the relatively large bubble velocities used in this work. The cross-sectional bubble shape is not axisymmetrical and cannot be obtained directly from images of the flow. Therefore, in this work, a mass balance-based model for Taylor flow is developed. It describes the gas hold-up as a function of bubble and liquid slug lengths, the number of bubbles formed per unit of time, the liquid superficial velocity, and the cross-sectional area of the bubbles relative to the channel cross-section. This model is applied to experimental data obtained by imaging techniques from which the dimensionless cross-sectional bubble area is determined. This allows for calculation of the gas hold-up, which is then shown to be a function of the flow quality according to Armand's experimentally obtained correlation [8]. The model presented in this work is similar, but not identical, to that of Thulasidas et al. [9]. The differences with the Thulasidas model will be addressed explicitly in the next section on Taylor flow model assumptions.

1.1. Taylor flow model assumptions

Before the Taylor flow model is described in detail, the main assumptions and their motivation are discussed.

(1) At any specific location in the channel, there is no variation in gas bubble and liquid slug sizes.
(2) There is a uniform, continuous liquid film surrounding the gas bubbles as well as the liquid circulation cells that form the liquid slugs.
(3) There is no flow in the liquid film.

Ad 1: For any single Taylor flow considered in this work, there is no variation in the amount of gas per bubble and the amount of liquid per slug. However, due to the pressure drop over the channel and the compressibility of the gas phase, the volume of a gas bubble varies with the location in the channel. The pressure dependence of the solubility of the gas phase in the liquid can also cause a small bubble volume change along the length of the channel, but this is not accounted for in this work. Thus, when considering a single location in the channel, all bubbles passing that location have the same volume for a given set of gas and liquid flow rates. Since there is no convective flow in or out of a liquid slug and the liquid phase is assumed to be incompressible all liquid slugs have the same volume for a given set of gas and liquid flow rates.

Ad 2: Up to certain values for the capillary number Ca, liquid circulation cells form between the gas bubbles. These liquid circulation cells are separated from the wall by a thin liquid film. Thus, the liquid film is not only present around the gas bubbles, but continues into the liquid slugs forming a uniform, continuous liquid film throughout the length of the channel. For capillaries with a square cross-section there is both theoretical and experimental evidence [1,2] that these circulation patterns exist for $Ca < 0.5$. For the experiments in channels with a rectangular cross-section described in this work, the capillary numbers are $Ca < 0.1$, and smaller than this threshold value. Even though the channels have a rectangular cross-section, it can be assumed that bypass flow does not occur and there is a continuous and uniform liquid film along the length of the channel.

Ad 3: The boundary conditions for the liquid flow in the film are: no shear stresses at the gas–liquid interface and no slip at the channel wall [2,9]. Shear between the gas bubble and the liquid film is therefore not a driving force for any flow in the film. It is also reported [2,6] that there is no pressure gradient in the liquid film in the uniform bubble region, eliminating another potential source for liquid flow in the film. For vertically oriented systems with respect to the gravity vector, gravity can cause flow in the film region, especially for channels with a rectangular cross-section. However, in this work horizontally oriented channels are used and the Bond number ($Bo = \rho g W_b^2/\sigma$) is in the order of 10^{-3}, so the effect of gravity is not significant. It is therefore assumed that there is no liquid flow in the film surrounding the gas bubbles. This is also assumed in the work of Thulasidas et al. [9] in the absence of gravity as a driving force.

Shear stress between the liquid in the slug and that in the film can induce flow in the film surrounding the liquid slug. Provided that the liquid slugs are longer than 1.5 times the channel diameter, this will result in fully developed laminar flow of the liquid at some point between two bubbles [1]. In the model developed by Thulasidas et al. [9] it is therefore assumed that there is a fully developed laminar flow in the liquid between two gas bubbles.

For thin films, the flow rate in the liquid film surrounding the liquid slug is a negligible fraction of the total flow rate. Therefore, in this work, it is assumed that the liquid film is stagnant and of equal thickness as the part of the liquid film surrounding the bubble. This is conceptually different from the assumption of Thulasidas et al. [1] and leads to a different derivation of the overall mass balance. For both models, continuity requires that the average velocity over the whole cross-sectional area of the channel is constant and is equal to the sum of the superficial gas and liquid velocities, regardless of the shape of the velocity profile in the slug and its surrounding liquid film. This condition is met for both models and thus, even though they are conceptually different, they lead to the same overall mass balance.

1.2. Taylor flow model development

In this work, a liquid slug is defined as the liquid present in the circulation cells and does not include any liquid present in the film. Once the static liquid film has been formed, the liquid flow consists solely out of the liquid in the slugs and there is no flow in or out of these slugs.

Since the liquid slugs are isolated packages of liquid moving through the same cross-sectional area A_b as the gas bubbles, their velocity is equal to the bubble velocity u_b. The overall velocity in the channel is the sum of the superficial gas U_g and liquid U_l velocities, which are based on the channel cross-sectional area A. Because the gas bubbles and liquid slugs move through what is effectively a channel with a smaller cross-sectional area A_b, the bubble velocity in the channel u_b is a factor A/A_b larger than the overall velocity in the channel:

$$u_b = \frac{A}{A_b}(U_g + U_l) \tag{1}$$

Now that all velocities have been defined, a mass balance can be made. A train of gas bubbles and liquid slugs is divided into unit cells consisting of one liquid slug, one gas bubble and the liquid film surrounding both the bubble and the slug (see Fig. 1).

The volume of one unit cell V_{uc} is equal to the cross-sectional area of the channel A multiplied by the sum of the bubble length L_b and the slug length L_s:

$$V_{uc} = A(L_b + L_s) \tag{2}$$

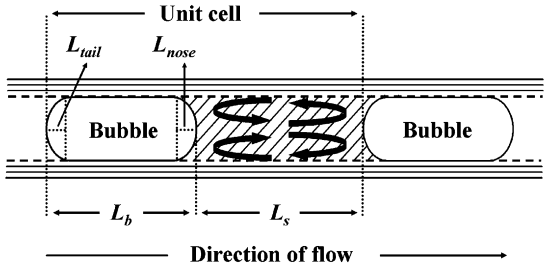

Fig. 1. Schematic of Taylor flow showing the definitions of the unit cell, bubble length L_b and the liquid slug length L_s. The lengths of the nose L_{nose} and tail L_{tail} sections of the bubble are also indicated. The diagonally dashed area is the liquid slug. The fluid circulation patterns relative to the bubble movement are also indicated. The horizontally dashed area indicates the uniform, static liquid film surrounding both the bubbles and the liquid slugs.

The volume of the liquid film in the unit cell V_f is then

$$V_f = (A - A_b)(L_b + L_s) \tag{3}$$

The volume of the liquid present in one liquid slug V_s is equal to the volumetric liquid flow rate divided by the slug frequency, which is equal to the bubble frequency F_b. The liquid in the liquid slug can be considered to consist of a part with volume $L_s A_b$ and the amount of liquid around the nose of the trailing and the tail of the leading gas bubbles. This volume is not known, but will depend on A_b. Assuming this volume is a linear function of A_b, then it can be written as $A_b\delta$, where δ is a correction on the liquid slug length to compensate for this extra volume. This gives

$$V_s = \frac{U_l A}{F_b} = A_b(L_s + \delta) \tag{4}$$

The volume of a gas bubble V_b is then the volume of the unit cell minus the volumes of the liquid slug and the liquid film in the unit cell. Combining Eqs. (2)–(4) gives

$$V_b = A_b(L_s + L_s) - \frac{U_l A}{F_b} \tag{5}$$

The gas hold-up ε_g in the unit cell is the gas bubble volume divided by the unit cell volume, giving

$$\varepsilon_g = \frac{A_b}{A} - \frac{U_l}{F_b(L_b + L_s)} = \frac{A_b}{A} - \frac{U_l}{u_b} \tag{6}$$

Apart from the liquid in the film, the liquid and the gas in one unit cell move with the bubble velocity u_b. This implies that adding the length of all unit cells passing a certain location per unit of time $F_b(L_b + L_s)$ gives the bubble velocity u_b.

Once the gas hold-up and the bubble velocity have been determined, the local superficial gas-velocity, U_g, can be calculated by

$$U_g = \varepsilon_g u_b \tag{7}$$

From the previous analysis it is clear that the cross-sectional bubble area is a key parameter for describing the hydrodynamics of Taylor flow and in particular for describing the gas hold-up.

2. Experimental

The micro fluidic chips used in this work were designed and constructed for investigating the influence of mixer design on the gas/liquid hydrodynamics in the subsequent channel as described in [10]. The chips consist of two anodically bonded borosilicate glass wafers. The micro fluidic structures were etched by deep reactive ion etching and the in- and outlet holes were made by powder blasting. Fig. 2 shows the designs of the mixers.

For both designs, the gas inlet is encompassed by two liquid inlets. The two mixers differ in angle at which the gas and liquid streams are contacted. For the cross mixer, the angle between the gas and liquid inlets is 90°. In the smooth mixer the inlets are nearly parallel to each other. Both mixers then focus the flow into a 2 cm long channel with a 50 μm × 100 μm rectangular cross-section.

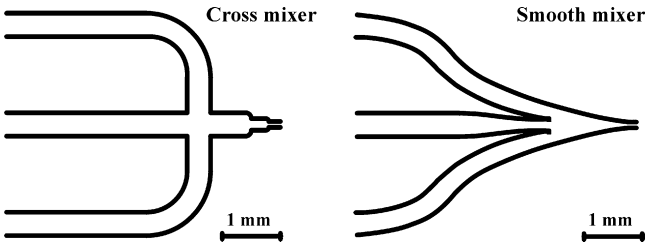

Fig. 2. Geometries of the two mixers used for realizing two-phase flow in a downstream channel with a rectangular cross-section of 100 μm × 50 μm and a length of 2 cm. The depth of these structures is 50 μm. The bar represents 1 mm.

Table 1
Superficial liquid U_l and gas velocities U_g for which a stable, regular Taylor flow was observed with bubble and slugs lengths suitable for image analysis

	U_l (m/s)	U_g (m/s)	$U_g/(U_g + U_l)$
Cross mixer	0.07–1.90	0.50–10	0.43–0.91
Smooth mixer	0.07–0.47	0.50–5.0	0.45–0.91

The superficial gas velocity is given at a temperature of 20 °C and a pressure of 1 bar. The range of flow qualities used in the experiments is also given.

All experiments were carried out with nitrogen gas and demineralised water at a temperature of 20 °C. The gas flow was regulated by a set of mass flow controllers (Bronkhorst F-200C and Bronkhorst F-201C). An LKB 2150 high-performance liquid chromatography pump was used to create the liquid flow. The range of superficial velocities for which a stable Taylor flow with bubble and slug lengths smaller than the length of the observation window was obtained, are given in Table 1.

Images of the flows were recorded by a Redlake MotionPro CCD camera connected to a Zeiss Axiovert 200 MAT inverted microscope. The images were recorded at a resolution of 1280 × 48 pixels at a rate of 10,000 frames per second. An exposure time of 12 μs was sufficient to eliminate significant motion blur. The width of one pixel represented 3.6 μm of channel length. All images captured 2.86 mm of channel length and their centerpoint was located 17.8 mm from the channel entrance. For every combination of gas and liquid velocities, three movies of 5000 frames each were recorded (0.5 s measurement time per movie).

For each movie, every individual bubble was tracked and its length was averaged over all frames it occurred in. These values were then averaged to obtain the average bubble length L_b for that movie. The same was done for the liquid slugs, giving the average slug length L_s. The bubble frequency F_b is the number of tracked bubbles divided by the measurement time. The average velocity of a single bubble was obtained by dividing the distance travelled by its centre of mass in the movie by the time that the bubble was present in that movie. Like the average bubble and slug lengths, the velocity was first determined for every single bubble and then averaged over all bubbles to give the average bubble velocity u_b.

3. Results and discussion

An expression for the liquid slug length L_s is obtained from Eq. (4). The liquid slug length is dependent on the amount of liquid in the slug and the dimensionless cross-sectional bubble area A_b/A:

$$L_s = \frac{U_l A}{F_b A_b} - \delta \tag{8}$$

In Fig. 3, the liquid slug length is plotted against U_l/F_b for both mixers.

From this figure it is clear that there is a linear relationship between these parameters. This implies that the dimensionless cross-sectional bubble area A_b/A, and thus the thickness of the liquid film, is constant for a wide range of bubble velocities, which was 0.24–7.12 m/s for the cross mixer and 0.54–4.44 m/s for the smooth mixer. The range of Weber numbers ($We = \rho W_b u_b^2/\sigma$) covered in this work is 0.06–50 indicating that inertial effects have a significant influence on the characteristics of the Taylor flow. The correction on the liquid slug length to compensate for the volume of liquid present around the nose and tail of a gas bubble δ is also obtained from the fit. The differences between the slopes of the curves and between the values of δ are

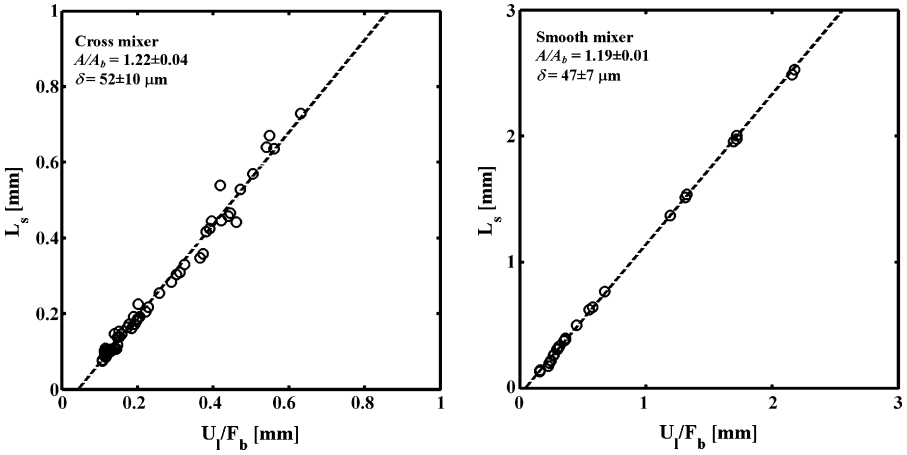

Fig. 3. The slug length L_s is plotted against the superficial liquid velocity U_l divided by the bubble frequency F_b for both the cross (left) and the smooth (right) mixers. The dotted line represents the linear fit according to Eq. (8). The values of the fitted parameters A/A_b and δ and their 95% confidence intervals are given in the figures.

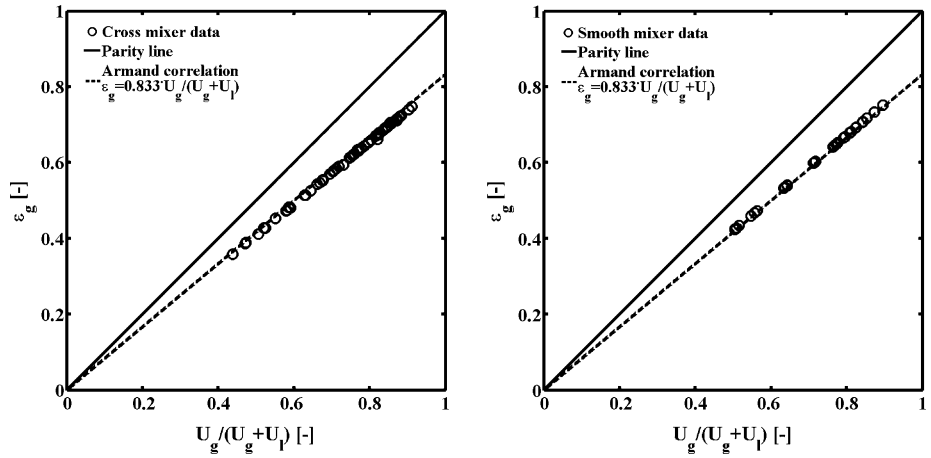

Fig. 4. The gas hold-up ε_g is plotted as a function of the flow quality $U_g/(U_g + U_l)$ for both the cross (left) and the smooth mixer (right). The Armand correlation is also plotted.

most likely due to experimental error. The larger spread in the data obtained with the cross mixer is the result of a less uniform bubble and slug size distribution for a given set of flow rates. This is caused by the differences in bubble formation mechanisms in the two mixers, as described in Haverkamp et al. [10].

The sum of the volumes occupied by the nose and tail of the gas bubble and the volume of the part of the liquid slug surrounding them is $A_b(L_{nose} + L_{tail})$. The length of the nose of the gas bubble is L_{nose} and the length of its tail is L_{tail}, as indicated in Fig. 1. The volume of liquid in this area is $A_b\delta$, so that the fraction of liquid in this volume is $\delta/(L_{nose} + L_{tail})$. For ease of calculation the shapes of the nose and tail sections of a bubble are assumed to be identical half ellipsoids with a cross-sectional area A_b. The total volume of the two halves is then $2A_b(L_{nose} + L_{tail})/3$ and $\delta/(L_{nose} + L_{tail})$ is 0.33. The lengths of the tails and noses of the gas bubbles have been estimated at both the largest and smallest bubble velocity used in this work. For these experiments the sum of the nose and tail lengths is 100 ± 10 μm and the value for $\delta/(L_{nose} + L_{tail})$ is then 0.5 ± 0.2. This is close to the value of 0.33 found if the nose and tail sections were shaped like half ellipsoids. It is concluded that a value for δ of 50 μm is realistic.

Laborie et al. [11] determined the relative bubble velocity $u_b/(U_g + U_l)$ for various gas/liquid systems. They used vertically oriented, glass capillaries with circular cross-sections with inner diameters of 1, 2, 3 and 4 mm. For every system, they found a constant relative bubble velocity, although the value varied with the gas/liquid system and the diameter of the capillary due to flow in the liquid film under the influence of gravity. The relative bubble velocity is equal to the inverse of the dimensionless cross-sectional bubble area (see Eq. (1)). Thus, the observation that the relative bubble velocity is constant is in accordance with the results in this work. Furthermore, the values of A/A_b obtained in this work are close to the value for the relative bubble velocity reported by Laborie et al. for an air/water system in a 1 mm capillary at a temperature of 20 °C, which is 1.24.

The gas hold-up was calculated from Eq. (6) using the fitted values for A/A_b. All other parameters in Eq. (6) were obtained experimentally. Eq. (7) was used to calculate the local superficial gas velocity from the measured bubble velocities and the gas hold-up. Fig. 4 shows the gas hold-up as a function of the flow quality for both mixers. The Armand correlation ($\varepsilon_g = 0.833U_g/(U_g + U_l)$ [8]) and the parity line are also plotted.

The Armand correlation was obtained for air/water Taylor flows in a horizontally oriented, smooth, brass tube with an inner diameter of 26 mm. The gas hold-up was estimated from the weight of the tube and was measured at various gas qualities. Correlating the two parameters resulted in the Armand correlation, $\varepsilon_g = 0.833U_g/(U_g + U_l)$, without addressing the physical interpretation of the constant [8].

In the analysis presented in this work, if Eq. (1) is substituted into Eq. (6), the following Eq. (9) is obtained:

$$\varepsilon_g = \frac{A_b}{A}\frac{U_g}{U_g + U_l} \tag{9}$$

Upon comparing Eq. (9) to the Armand correlation, the constant 0.833 in their correlation can be considered to be the dimensionless cross-sectional bubble area A_b/A in his experiments. This value is close to the values obtained for A_b/A in this work: 0.82 for the cross mixer and 0.84 for the smooth mixer. Chung and Kawaji [12] obtained similar linear relationships for a nitrogen/water flow in glass capillaries of circular cross-section with diameters of 500 and 251 μm. However, for smaller diameters (100 and 50 μm) they obtained a non-linear relationship between the gas hold-up and flow quality, which is not confirmed by the data in this work at similar channel diameters. Chung and Kawaji [12] suggested that the difference in their results for the various channel diameters might be due to limitations of their set-up. For large bubble velocities and liquid hold-ups in the 100 and 50 μm channels, it might be possible that their imaging system does not capture all the bubbles passing the measurement location, thus underestimating the gas hold-up. Serizawa et al. [13] have verified the Armand correlation for an air/water flow in a silica capillary of circular cross-section with an internal diameter of 20 μm.

The validity of the Armand correlation in both this work and in literature for horizontal air/water and nitrogen/water Taylor flows implies that the liquid film thickness occupies a fixed fraction of the channel cross-section over a wide range of chan-

nel diameters and bubble velocities. This is in agreement with the qualitative analysis of Aussillous et al. [5] that, for Taylor flows with significant inertial effects, the liquid film thickness converges to a fixed fraction of the channel width.

4. Conclusions

The conditions in small reactor channels operated under Taylor flow are often such that inertial effects cannot be ignored so that classical lubrication theory can no longer be used for estimating the liquid film thickness. Therefore, in this work, the gas hold-up and its relation to the liquid film thickness are studied under conditions where inertial effects are significant.

A mass balance-based model for Taylor flow without flow in the liquid film is developed. A uniform, stagnant liquid film surrounding both the gas bubbles and the liquid circulation cells is the main assumption in this model.

Experimental data are obtained for a nitrogen/water system and bubble velocities range from 0.24 to 7.12 m/s. The gas hold-up is obtained by applying the model to the experimental data. The gas hold-up as a function of flow quality follows Armand's experimentally obtained correlation.

The model shows that the validity of the Armand correlation implies that the liquid film thickness is not dependent on the bubble velocity. In literature, the Armand correlation is also obtained for nitrogen/water and air/water Taylor flows for a wide range of bubble velocities and channel diameters. This indicates that the liquid film thickness is not only independent of the bubble velocity, but also occupies a fixed fraction of the channel cross-section independent of the channel diameter.

Acknowledgements

The financial support by the Dutch Technology Foundation (STW, project no. EPC.6359), Organon, DSM, Shell, Akzo Nobel Chemicals, Bronkhorst High-Tech and TNO is gratefully acknowledged.

References

[1] T.C. Thulasidas, M.A. Abraham, R.L. Cerro, Flow patterns in liquid slugs during bubble-train flow inside capillaries, Chem. Eng. Sci. 52 (17) (1997) 2947–2962.
[2] W.B. Kolb, R.L. Cerro, The motion of long bubbles in tubes of square cross section, Phys. Fluids A 5 (7) (1993) 1549–1557.
[3] G. Berčič, A. Pintar, The role of gas bubbles and liquid slug lengths on mass transport in the Taylor flow through capillaries, Chem. Eng. Sci. 52 (21–22) (1997) 3709–3719.
[4] F.P. Bretherton, The motion of long bubbles in tubes, J. Fluid. Mech. 10 (1961) 166–188.
[5] P. Aussillous, D. Quere, Quick deposition of a fluid on the wall of a tube, Phys. Fluids 12 (10) (2000) 2367–2371.
[6] M.T. Kreutzer, F. Kapteijn, J.A. Moulijn, C.R. Kleijn, J.J. Heiszwolf, Inertial and interfacial effects on pressure drop of Taylor flow in capillaries, AIChE J. 51 (9) (2005) 2428–2440.
[7] M. Heil, Finite Reynolds number effects in the Bretherton problem, Phys. Fluids 13 (9) (2001) 2517–2521.
[8] A.A. Armand, The resistance during the movement of a two-phase system in horizontal pipes, Izv. Vses. Teplotekh. Inst. 1 (1946) 16–23.
[9] T.C. Thulasidas, M.A. Abraham, R.L. Cerro, Bubble-train flow in capillaries of circular and square cross section, Chem. Eng. Sci. 50 (2) (1995) 183–199.
[10] V. Haverkamp, V. Hessel, H. Löwe, G. Menges, M.J.F. Warnier, E.V. Rebrov, M.H.J.M. De Croon, J.C. Schouten, M.A. Liauw, Hydrodynamics and mixer-induced bubble formation in micro bubble columns with single and multiple channels, Chem. Eng. Technol. 29 (9) (2006) 1015–1026.
[11] S. Laborie, C. Cabassud, L. Durand-Bourlier, J.M. Lainé, Characterisation of gas–liquid two-phase flow inside capillaries, Chem. Eng. Sci. 54 (23) (1999) 5723–5735.
[12] P.M.Y. Chung, M. Kawaji, The effect of channel diameter on adiabatic two-phase flow characteristics in microchannels, Int. J. Multiphase Flow 30 (7–8) (2004) 735–761.
[13] A. Serizawa, Z. Feng, Z. Kawara, Two-phase flow in microchannels, Exp. Therm. Fluid Sci. 26 (6–7) (2002) 703–714.